ACTA SCIENTIARUM POLONORUM
aspa.sggw.edu.pl
Acta Sci. Pol.
Architectura 23 (2024), 264–273
ISSN 1644-0633 (suspended) eISSN 2544-1760 DOI: 10.22630/ASPA.2024.23.20

ORIGINAL PAPER

Received: 15.05.2024
Accepted: 01.07.2024

AN ANALYSIS OF THE SUPPRESSION OF A PAIR OF ODD AND EVEN TEMPERATURE FLUCTUATION IN AN AREA OCCUPIED BY A TWO-PHASE ONE-DIRECTIONAL PERIODICALLY LAYERED COMPOSITE

Łukasz Wodzyński✉, Dorota Kula, Ewaryst Wierzbicki

Institute of Civil Engineering, Warsaw University of Life Sciences – SGGW, Warsaw, Poland

ABSTRACT

The study concerns a heat conduction problem in a two-phase, one-directional periodically layered composite (commonly referred to as a laminate). The model is strictly related to considerations regarding continuous media and was introduced by Professor Czesław Woźniak. The basis for the study is a re-formulation of the heat conduction model for composites, referred to in the literature as "the extended tolerance heat conduction model". The model equations consider coefficients responsible for the intensity of exponential and rotational suppression of boundary fluctuations of a temperature field in a limited area or in a half-space occupied by the composite. The study investigated the dependence of the suppression intensity of boundary fluctuations on the geometrical and material properties of the composite. Three special cases of pairs of interacting boundary fluctuations were analysed.

Keywords: effective heat conduction, periodic composite, boundary effect, extended tolerance model

INTRODUCTION

Composite materials, due to their insulating properties, are widely used to protect certain rooms from the harmful effects of thermal fields and resulting displacement fields. Thermal loads acting on composite materials cause fluctuations in the temperature field at the boundaries. This results in the formation of a so-called "near-boundary layer" (similar to a boundary layer in fluid mechanics) on both sides of a composite baffle, as if the ambient temperature automatically adjusts to the non-homogeneous structure of the composite. The boundary fluctuations that occur in this way are suppressed within the baffle during heat transport through the composite area. The movement of the boundary temperature impulse through the composite baffle is subject to two types of reactions: exponential suppression and rotational suppression (i.e., pulsations perpendicular to the baffle wall). The intensities of these two suppressions are functions of a quotient of conductivities $\kappa = k_{II}/k_{I}$ and a saturation of one of the components η. The periodic composites ensure the best suppression of disturbances in directions perpendicular to a periodicity direction.

Łukasz Wodzyński https://orcid.org/0000-0002-4924-5784; Dorota Kula https://orcid.org/0000-0002-7445-2822;
Ewaryst Wierzbicki https://orcid.org/0000-0001-8991-536X
✉lukasz_wodzynski@sggw.edu.pl

The aim of the paper is to attempt a description of the relationship between the suppression of fluctuation intensity in directions perpendicular to the periodicity direction and the internal structure of the composite. The results of the study on the boundary effect should contribute to designing composites with the best insulation properties. The boundary effect can be understood, in general, as the influence of boundary conditions on physical phenomena occurring in the composite. The analysis of this effect is strictly related to the fact that the equations of thermoelasticity contain components with a second spatial derivative. The analysis of the boundary effect in this study is restricted merely to heat conduction described by Fourier's conduction law. The extended tolerance model, applied here, has been described and used in many works (Kula, Mazewska & Wierzbicki, 2012; Kula, 2016; Kula, Wierzbicki, Witkowska-Dobrev & Wodzyński, 2018; Wierzbicki, Kula & Wodzyński, 2018a; Wierzbicki, Kula & Wodzyński, 2018b; Kula & Wodzyński, 2020; Wodzyński, Kula & Wierzbicki, 2018). The approach to the boundary effect phenomenon, described in this study, has also been applied in research works using methods similar to the tolerance averaging technique (Kula, 2015; Szlachetka & Wągrowska, 2011; Witkowska-Dobrev & Wągrowska, 2015).

Fundamentals of tolerance modelling, which were used to derive the equations used in the present study, have been presented in the monograph by Wierzbicki and Woźniak (2000). The mathematical theory of tolerance modelling was developed by Ostrowski (2017). To capture the boundary effect, the study made use of results obtained by Wierzbicki (2019) and Kula and Wierzbicki (2019).

DESCRIPTION OF THE MODEL OF THE PHENOMENON AND THE METHODS USED

For the sake of simplification, it was assumed that the area occupied by the composite was a cuboid (Fig. 1). The axis OY determines the direction of periodicity. The temperature field θ inside the area is evoked by two constant temperature values: inside and outside the room. Moreover, the temperature field does not depend on time and is a function of geometrical variables (y, z). In this model, it was also assumed that the heat flux vector was continuous in the direction perpendicular to interfaces between the components of the composite and that the components themselves were isotropic. Such conditions of heat conduction are mathematically expressed by a boundary problem for the parabolic equation of heat conduction:

$$\rho c \dot{\theta} - \nabla^T [K \nabla \theta] = 0, \tag{1}$$

where the symbols K, ρ and c represent respectively: heat conductivity matrix, mass density field and specific heat field.

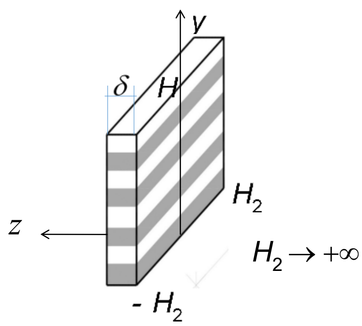

Fig. 1. Two-phase one-directional periodic composite

Source: own work.

Further considerations concern an analysis of the phenomenon of the transport of a pair of two interacting fluctuations, odd and even, through the composite. The Fourier's fluctuations under consideration are sums of products of Fourier's amplitudes a_1 and a_2 with related shape functions, also referred to as impulses. These temperature impulses are defined by the formulas (2) and formulas (13):

$$f_{EVEN}(\nu_1,y)=\begin{cases}-\dfrac{\lambda}{2}\alpha_1-\dfrac{\lambda}{2}\alpha_1\cos\left(\dfrac{2\pi\nu_1}{\lambda\eta_{\mathrm{I}}}y+2\pi\nu_1\right) & \text{for } -\lambda\eta_{\mathrm{I}}\le y\le 0 \quad \alpha_1=\dfrac{1}{\eta_{\mathrm{I}}}\\ \dfrac{\lambda}{2}\alpha_2+\dfrac{\lambda}{2}\alpha_2\cos\left(\dfrac{2\pi\nu_1}{\lambda\eta_{\mathrm{II}}}y-2\pi\nu_1\right) & \text{for } 0\le y\le\lambda\eta_{\mathrm{II}} \quad \alpha_2=\dfrac{1}{\eta_{\mathrm{II}}}\end{cases}$$
$$f_{NP}(\nu_2,y)=\begin{cases}-\dfrac{\lambda}{2}\cos\left(\dfrac{(2\nu_2-1)\pi}{\lambda\eta_{\mathrm{I}}}y+(2\nu_2-1)\pi\right) & \text{for } -\lambda\eta_{\mathrm{I}}\le y\le 0\\ -\dfrac{\lambda}{2}\cos\left(\dfrac{(2\nu_2-1)\pi}{\lambda\eta_{\mathrm{II}}}y-(2\nu_2-1)\pi\right) & \text{for } 0\le y\le\lambda\eta_{\mathrm{II}}\end{cases} \tag{2}$$

The parameter ν assumes positive integer values. A mean of each of the impulses within the individual cell must be equal to 0: $\langle f_{EVEN}(\nu_1,y)\rangle = \langle f_{ODD}(\nu_2,y)\rangle = 0$. It is also a criterion for determining the coefficients a_1 and a_2.

The averaging operation, applied here, is defined by the formula:

$$\langle f\rangle=\frac{1}{l^{\mathrm{I}}+l^{\mathrm{II}}}\int_{-l^{\mathrm{I}}}^{l^{\mathrm{II}}} f(y)dy. \tag{3}$$

The amplitudes of the fluctuations can only be determined if the analysed pairs of impulses create an orthogonal Fourier's basis (i.e., a definite integral of the product of impulses within an area of a simple cell is equal to zero). The impulses (2) are mutually orthogonal, so there is no need to "orthogonalise" them. These impulses act as tolerance shape functions in the extended tolerance model used in this study to examine the transportation of fluctuations through a periodic composite. In this model, the equations of heat conduction have the form (Kula & Wodzyński, 2020):

$$\begin{aligned}&\langle c\rangle\dot{u}-\nabla^T(\langle k\rangle\nabla u+\langle k\nabla^T\varphi^p\rangle a_p)=-\langle b\rangle,\\ &\lambda^2(A_c^{pq}\dot{a}_q-\nabla_z{}^T A_k^{pq}\nabla_z a_q)+2\lambda s^{pq}\nabla_z a_q+\{k\}^{pq}a_q=(L_a^{\lambda}[u])^p\end{aligned} \tag{4}$$

and are binding in materially homogeneous parts of the area $\boldsymbol{\Omega}$ occupied by the composite, wherein:

$$\{k\}^{pq}=\langle\nabla_y{}^T\varphi^p k\nabla\varphi^q\rangle,\quad 2s^{pq}=\langle\nabla_y{}^T\varphi^p k\varphi^q\rangle-\langle\nabla^T\varphi^q k\varphi^p\rangle. \tag{5}$$

In Eq. $(4)_2$, next to the derivatives of the highest order, there are coefficients $A_c^{pq}\equiv\langle\varphi^p c\varphi^q\rangle$, $A_k^{pq}\equiv\langle\varphi^p k\varphi^q\rangle$. The expression $(L_a^{\lambda}[u])^p$ in the right side of Eq. $(4)_2$ includes all averaged expressions containing heat sources. In Eq. (4):

- u represents the average temperature field;
- a_p represents the Fourier's amplitudes;
- k represents the effective conductivity matrix;
- c represents the specific heat field;
- φ^p, φ^q represents the coefficients constituting an orthogonal Fourier's basis.

Furthermore, Eq. (4) contains a scale parameter equal to a quotient of a characteristic length λ of the repeatable cell to a characteristic length of the area occupied by the composite. The symbol ∇_y is a denotation of the gradient operator $\nabla \equiv [\partial_1, \partial_2, \partial_3]^T$ related to the directions of periodicity and the formula $\nabla \equiv \nabla_z + \nabla_y$ specifies a projection ∇_z of the gradient operator on directions perpendicular to the directions of periodicity. The summation convention holds. Eq. $(4)_2$ is called the 'equation of boundary effect phenomenon'. For the pair of impulses given in formulas (2), the equation of boundary effect phenomenon assumes the form:

$$\frac{d^4a}{dz^4}+\frac{1}{\lambda^2}\left(\frac{4d^2}{\gamma_1\gamma_2}-\frac{\langle k\rangle_H}{\langle k\rangle}\left(\frac{c_1}{\gamma_1}+\frac{c_2}{\gamma_2}\right)\right)\frac{d^2a}{dz^2}+\frac{1}{\lambda^4}\left(\frac{\langle k\rangle_H}{\langle k\rangle}\right)^2\frac{c_1c_2}{\gamma_1\gamma_2}a=0. \tag{6}$$

In this equation, a represents both the amplitude a_1 and a_2. The individual coefficients are given as:

$$\begin{aligned}
&\gamma_1=\frac{\langle kf_{EVEN}f_{EVEN}\rangle}{\langle k\rangle},\quad \gamma_2=\frac{\langle kf_{ODD}f_{ODD}\rangle}{\langle k\rangle},\\
&c_1=\frac{\langle k\nabla f_{EVEN}\nabla f_{EVEN}\rangle}{\langle k\rangle},\quad c_2=\frac{\langle k\nabla f_{ODD}\nabla f_{ODD}\rangle}{\langle k\rangle},\\
&d=\frac{\langle kf_{EVEN}\nabla f_{ODD}\rangle-\langle k\nabla f_{EVEN}f_{ODD}\rangle}{\langle k\rangle},
\end{aligned} \tag{7}$$

wherein $\langle k\rangle=\eta_I k^I+\eta_{II}k^{II}$. The characteristic equation for Eq. (6) is a biquadratic equation:

$$R^4+\frac{1}{\lambda^2}\left(\frac{4d^2}{\gamma_1\gamma_2}-\frac{\langle k\rangle_H}{\langle k\rangle}\left(\frac{c_1}{\gamma_1}+\frac{c_2}{\gamma_2}\right)\right)R^2+\frac{1}{\lambda^4}\left(\frac{\langle k\rangle_H}{\langle k\rangle}\right)^2\frac{c_1\cdot c_2}{\gamma_1\gamma_2}=0, \tag{8}$$

which can be transformed into a quadratic characteristic equation by changing the variables $r = R^2$:

$$r^2+\frac{1}{\lambda^2}\left(\frac{4d^2}{\gamma_1\gamma_2}-\frac{\langle k\rangle_H}{\langle k\rangle}\left(\frac{c_1}{\gamma_1}+\frac{c_2}{\gamma_2}\right)\right)r+\frac{1}{\lambda^4}\left(\frac{\langle k\rangle_H}{\langle k\rangle}\right)^2\frac{c_1c_2}{\gamma_1\gamma_2}=0,\quad r=R^2, \tag{9}$$

where $\langle k\rangle_H=\dfrac{k^I k^{II}}{\eta_I k^{II}+\eta_{II}k^I}$. The discriminant of Eq. (9) is given as:

$$\Delta\equiv\frac{1}{\lambda^4}\left[\frac{4d^2}{\gamma_1\gamma_2}-\frac{\langle k\rangle_H}{\langle k\rangle}\left(\frac{c_1}{\gamma_1}+\frac{c_2}{\gamma_2}\right)\right]^2-4\cdot\frac{1}{\lambda^4}\left(\frac{\langle k\rangle_H}{\langle k\rangle}\right)^2\frac{c_1\cdot c_2}{\gamma_1\gamma_2}. \tag{10}$$

The roots of the characteristic equation are four complex numbers r_1, r_2, r_3 and r_4, for which the minimum absolute value of the real part $\omega_{\exp}$, as well as the minimum absolute value of the imaginary part ω_{rot}, are interpreted in this contribution as exponential intensity and rotational intensity respectively. The exponential intensity $\omega_{\exp}$ depends on the thermal resistance exerted by the conductor and the velocity of suppression of the fluctuations. The rotational intensity ω_{rot} expresses the velocity of trigonometric fluctuations. Both of these intensities, created by the impulses (2), can be calculated using the following formulas:

– for $\Delta \geq 0$:

$$\omega=\sqrt{\frac{1}{2}\left\{\frac{1}{\lambda^2}\frac{\langle k\rangle_H}{\langle k\rangle}\left[\left(\frac{c_1}{\gamma_1}+\frac{c_2}{\gamma_2}\right)-\frac{4d^2}{\gamma_1\gamma_2}\right]+\sqrt{\Delta}\right\}}, \tag{11}$$

– for $\Delta < 0$:

$$\omega_{\mathrm{exp}} = \frac{1}{2}\sqrt{\frac{1}{\lambda^2}\left(\frac{\langle k\rangle_H}{\langle k\rangle}\left(\frac{c_1}{\gamma_1}+\frac{c_2}{\gamma_2}\right)-\frac{4d^2}{\gamma_1\gamma_2}\right)+\sqrt{\left[\frac{1}{\lambda^2}\left(\frac{4d^2}{\gamma_1\gamma_2}-\frac{\langle k\rangle_H}{\langle k\rangle}\left(\frac{c_1}{\gamma_1}+\frac{c_2}{\gamma_2}\right)\right)\right]^2-\Delta}},$$

$$\omega_{\mathrm{rot}} = \sqrt{\frac{-\Delta}{\frac{1}{\lambda^2}\left(\frac{\langle k\rangle_H}{\langle k\rangle}\left(\frac{c_1}{\gamma_1}+\frac{c_2}{\gamma_2}\right)-\frac{4d^2}{\gamma_1\gamma_2}\right)+\sqrt{\left[\frac{1}{\lambda^2}\left(\frac{4d^2}{\gamma_1\gamma_2}-\frac{\langle k\rangle_H}{\langle k\rangle}\left(\frac{c_1}{\gamma_1}+\frac{c_2}{\gamma_2}\right)\right)\right]^2-\Delta}}}. \qquad (12)$$

If the expression inside the square root in (11) is not negative, then (11) represents the exponential intensity and the rotational intensity is 0. However, if the expression inside the square root in (11) is negative, then (11) describes two conjugated imaginary numbers, with the positive one being the rotational intensity. The graphs below present the dependences of the exponential and rotational intensity on the parameters κ and η, where κ represents the quotient of conductivities of the components and η means a share of one of these components in the whole volume.

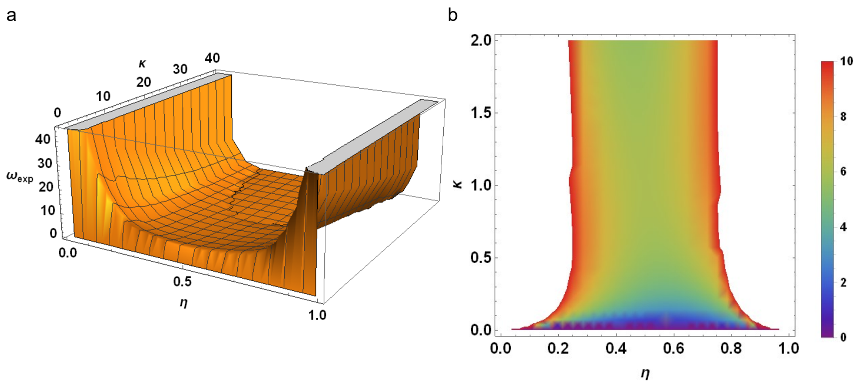

Fig. 2. Graphs for the pair of impulses (2): a – 3D graph of the exponential intensity; b – colour map for the exponential intensity within the range (0, 10)

Source: own work.

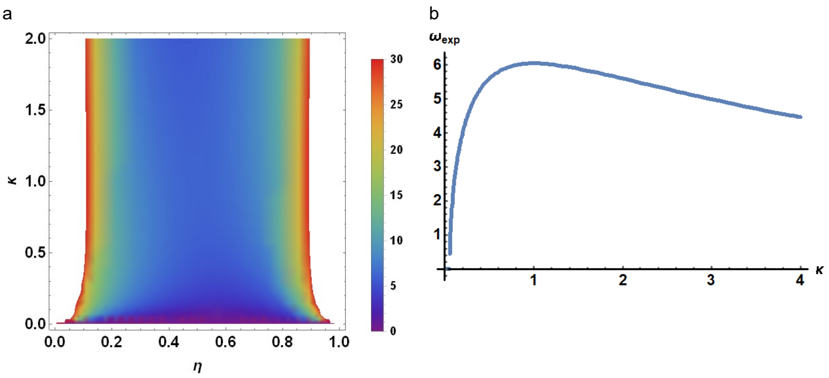

Fig. 3. Graphs for the pair of impulses (2); a – colour map for the exponential intensity within the range (0, 30); b – the exponential intensity for $\eta = 0.5$

Source: own work.

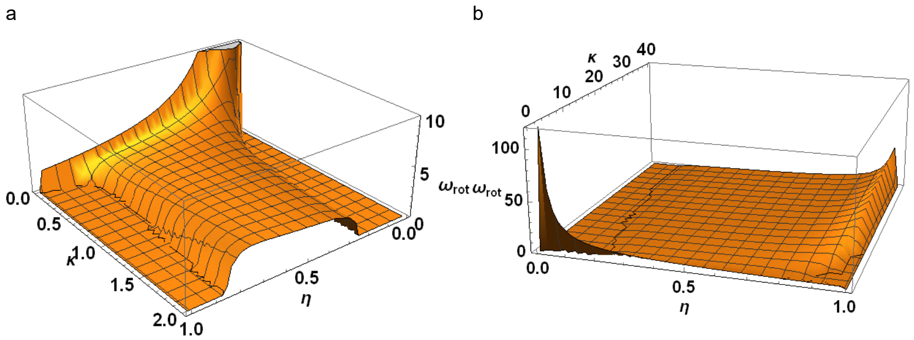

Fig. 4. 3D graphs of the rotational intensity for the pair of impulses (2): a – within the range (0, 10); b – within the range (0, 100) for κ varying from 0 to 40

Source: own work.

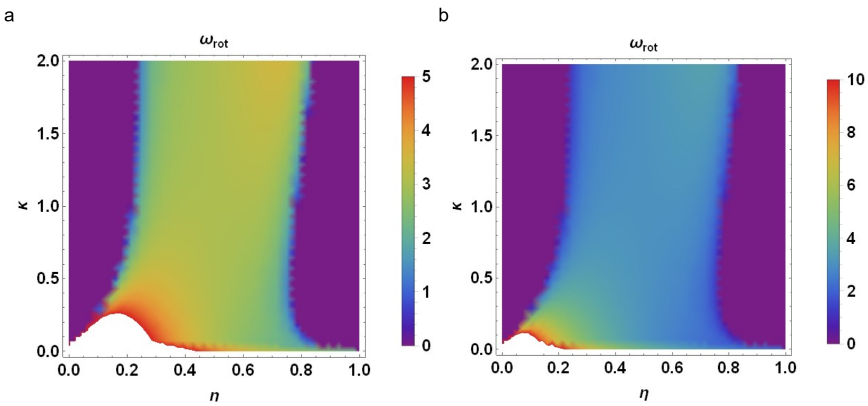

Fig. 5. Colour maps for the rotational intensity within the ranges: a – (0, 5); b – (0, 10)

Source: own work.

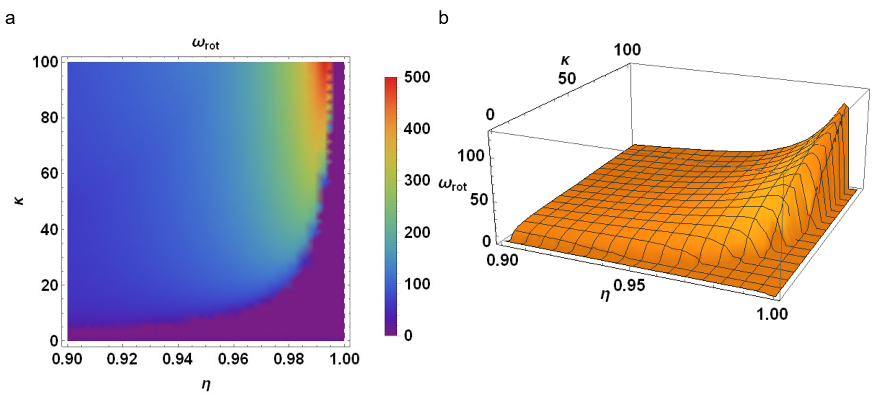

Fig. 6. Graphs of the rotational intensity for the pair of impulses (2) in the range accentuating a characteristic ridge

Source: own work.

In Figure 3b, the graph line is broken because the one-sided limit of this intensity is infinite in this point. A similar situation is for the function $y = \sqrt{x}$ in the point $x = 0$. A single point of indifferentiability corresponds to the condition $\Delta = 0$. The singularity occurs for $\kappa \approx 0.058$. The 3D graphs of the rotational and exponential intensities suggest that the highest suppression intensity occurs for an almost homogeneous structure of the baffle.

Interesting conclusions can be drawn after an analysis of suppression of the pair of impulses given by the formulas:

$$
\begin{gathered}
f_{EVEN}(\nu_1, y) = \begin{cases} -\dfrac{\lambda}{2}\alpha_1 - \dfrac{\lambda}{2}\alpha_1 \cos\left(\dfrac{2\pi\nu_1}{\lambda\eta_{\mathrm{I}}} y + 2\pi\nu_1\right) & \text{for } -\lambda\eta_{\mathrm{I}} \le y \le 0 \quad \alpha_1 = \dfrac{1}{\eta_{\mathrm{I}}} \\ \dfrac{\lambda}{2}\alpha_2 + \dfrac{\lambda}{2}\alpha_2 \cos\left(\dfrac{2\pi\nu_1}{\lambda\eta_{\mathrm{II}}} y - 2\pi\nu_1\right) & \text{for } 0 \le y \le \lambda\eta_{\mathrm{II}} \quad \alpha_2 = \dfrac{1}{\eta_{\mathrm{II}}} \end{cases} \\
f_{ODD}(\nu_1, y) = \begin{cases} f_{ODD}(\nu_2, y) + \beta f_{EVEN}(\nu_1, y) & \text{for } -\lambda\eta_{\mathrm{I}} \le y \le 0 \quad \alpha_1 = \dfrac{1}{\eta_{\mathrm{I}}} \\ f_{ODD}(\nu_2, y) + \beta f_{EVEN}(\nu_1, y) & \text{for } 0 \le y \le \lambda\eta_{\mathrm{II}} \quad \alpha_2 = \dfrac{1}{\eta_{\mathrm{II}}} \end{cases}.
\end{gathered} \tag{13}
$$

The impulses $f_{EVEN}(\nu_1, y)$ and $f_{ODD}(\nu_2, y)$ have been previously defined. The equation of boundary effect is still fulfilled; the previously calculated coefficients γ_1, c_1 and d remain unchanged. However, the coefficients γ_2 and c_2 change:

$$
\gamma_2 = \frac{\langle k f_{ODD} f_{ODD} \rangle}{\langle k \rangle}, \quad c_2 = \frac{\langle k \nabla f_{ODD} \nabla f_{ODD} \rangle}{\langle k \rangle}. \tag{14}
$$

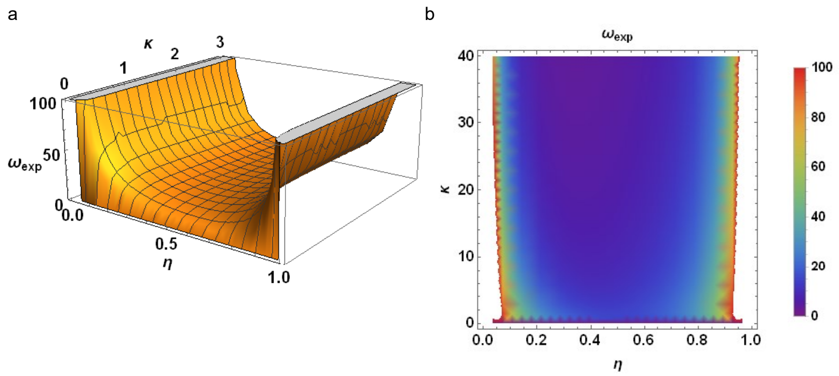

Fig. 7. Exponential intensity for the pair of impulses (13): a – 3D graph; b – colour map

Source: own work.

In a special case, when $\dfrac{c_1}{\gamma_1} = \dfrac{c_2}{\gamma_2}$ and $\beta \to \infty$, the roots of the characteristic equation are equal to:

$$
R = \sqrt{\frac{4}{3} \cdot \frac{\langle k \rangle_H}{\langle k \rangle} \frac{(\pi\nu_1)^2}{\lambda^4} \cdot \frac{\left[\dfrac{k_{\mathrm{I}}}{\eta_{\mathrm{I}}^3} + \dfrac{k_{\mathrm{II}}}{\eta_{\mathrm{II}}^3}\right]}{\left[\dfrac{k_{\mathrm{I}}}{\eta_{\mathrm{I}}} + \dfrac{k_{\mathrm{II}}}{\eta_{\mathrm{II}}}\right]}} \ \vee \ R = -\sqrt{\frac{4}{3} \cdot \frac{\langle k \rangle_H}{\langle k \rangle} \frac{(\pi\nu_1)^2}{\lambda^4} \cdot \frac{\left[\dfrac{k_{\mathrm{I}}}{\eta_{\mathrm{I}}^3} + \dfrac{k_{\mathrm{II}}}{\eta_{\mathrm{II}}^3}\right]}{\left[\dfrac{k_{\mathrm{I}}}{\eta_{\mathrm{I}}} + \dfrac{k_{\mathrm{II}}}{\eta_{\mathrm{II}}}\right]}}. \tag{15}
$$

The characteristic equation in this case has four real roots with equal modules and different signs. The positive part of these roots represents the desired exponential intensity. The rotational intensity is equal to 0.

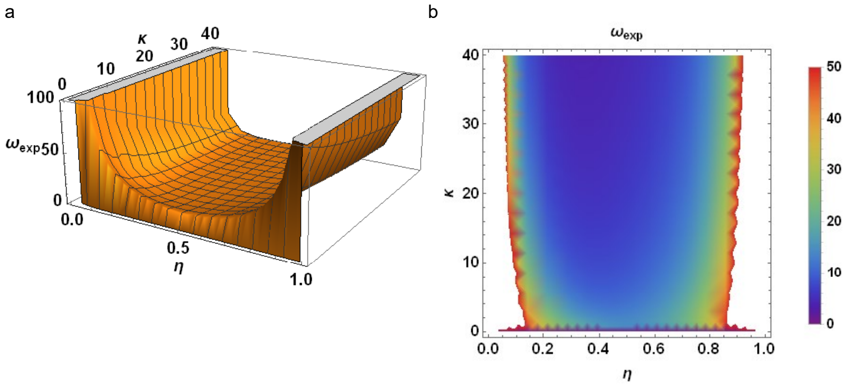

Fig. 8. Exponential intensity for the pair of impulses (13) for $\frac{c_1}{\gamma_1} = \frac{c_2}{\gamma_2}$ and $\beta \to \infty$: a – 3D graph; b – colour map

Source: own work.

SUMMARY AND CONCLUSIONS

In the study, appropriate formulas for two types of intensity in selected cases of fluctuation boundary loads were applied. Only the analysis of the suppression of pairs of fluctuations was conducted. The authors of this study are not familiar with the formal procedures for determining the critical points of the functions $\omega_{exp}(\kappa, \eta)$ and $\omega_{rot}(\kappa, \eta)$ in the case of pairs of fluctuations for which the set of two ordinary differential equations describing the boundary effect phenomenon transforms into a single fourth order equation, as it occurs in the cases being analysed in this study. Searching for the values of κ and η, for which the fluctuation suppression intensities reach extremely high values, is only possible in a numerical way and, therefore, it was the aim of the graphs obtained using computer programs and presented in this study. In order to better illustrate the results, colour maps for different parameter ranges (κ, η) were used in addition to the traditional graphs.

Based on a visual analysis of these graphs, one can state that the exponential suppression is the highest if η approaches 0 or infinity. Such a situation occurs when the baffle is almost homogeneous (the share of one of the components is close to 0), as well as in areas in the neighbourhood of the interface between the composite components. In the case of the rotational intensity for the first of the investigated pairs of fluctuations, the phenomenon is opposite to some extent – the rotational intensity is higher for the middle values of η. Certainly, the highest values of the rotational intensity occur in the neighbourhood of the point (0, 0). Moreover, if conductivities of the composite components are highly diversified (κ > 20), a distinct ridge of the rotational intensity exists within the range η = (0.9, 1). This characteristic has not been illustrated or recognised in any of the previous studies on the subject. With regard to the argument κ, the maximum of the exponential suppression for both of the pairs of impulses exists within the range κ = (0.4, 1).

The last of the discussed cases – the impulses (13) for $\beta \to \infty$ – can be of great importance in the mechanics, particularly in civil engineering: it suggests a set of fluctuations creating a relatively small threat of destruction of precise electronical devices placed in rooms whose walls are built of composite materials. In this case, the limit value of the rotational intensity is equal to 0, and the exponential suppression can be controlled by the saturation values of the composite components. A laboratory verification of the obtained results seems to be possible only after transporting considerations onto the area of hyperbolic heat conduction or linear elasticity within the frames of wave analysis.

As a principal achievement of this study, it can be acknowledged that an identification of interacting fluctuations, both odd and even, was made. These fluctuations had unlimited amplitude and did not cause any damage to a device placed inside of a room with walls made of a composite material. The rotational intensity approached 0 after the limit transition of the parameter β to infinity. The exponential intensity was able to be controlled by a saturation parameter of one of the components of a two-phase composite.

Authors' contributions

Conceptualisation: E.W.; methodology: E.W., D.K. and Ł.W.; validation: D.K. and Ł.W.; formal analysis: D.K. and Ł.W.; investigation: E.W., D.K. and Ł.W.; resources: D.K. E.W.; writing – original draft preparation: Ł.W., writing – review and editing: Ł.W., D.K. and E.W.; visualisation: Ł.W., supervision: E.W. and D.K.

All authors have read and agreed to the published version of the manuscript.

REFERENCES

Kula, D. (2015). On the existence of the sinusoidal-type temperature fluctuations which are independently suppressed by the periodic two-phased conducting layer. *Acta Scientiarum Polonorum. Architectura*, *14* (4), 5–12.

Kula, D. (2016). *Fourier variant homogenization of the heat transfer processes in periodic composites* (doctoral thesis). Lodz University of Technology, Łódź.

Kula, D., Mazewska, M. & Wierzbicki, E. (2012). Some remarks on the tolerance averaging of heat conduction in chessboard palisade-type periodic composites. *Przegląd Naukowy. Inżynieria i Kształtowanie Środowiska*, *21* (3), 131–140.

Kula, D. & Wierzbicki, E. (2019). Surface localized heat transfer in periodic composites. *Acta Mechanica et Automatica*, *13* (2), 124–129.

Kula, D., Wierzbicki, E., Witkowska-Dobrev, J. & Wodzyński, Ł. (2018). Fourier Variant Homogenization Treatment of Single Impulse Boundary Effect Behaviour. *Mechanics & Mechanical Engineering*, *22* (3), 683–690.

Kula, D. & Wodzyński, Ł. (2020). Transfer of thermal fluctuations through the building partition formed by periodic composite material. *Acta Scientiarum Polonorum. Architectura*, *19* (1), 21–30.

Ostrowski, P. P. (2017). *Tolerance modelling of thermomechanics in microstructured media*. Lodz: Lodz University of Technology Press.

Szlachetka, O. & Wagrowska, M. (2011). Efekt brzegowy w warstwowej przegrodzie o podłużnej gradacji własności. *Acta Scientiarum Polonorum. Architectura*, *10* (3), 27–34.

Wierzbicki, E. (2019). *Averaging techniques in thermomechanics of Composite Solids*. *Surface Localization versus Tolerance Averaging.* Warsaw: University of Life Sciences Press.

Wierzbicki, E., Kula, D. & Wodzyński, Ł. (2018a). Effective macroscopic description for heat conduction in periodic composites. *AIP Conference Proceedings*, *1922* (1), 140004. https://doi.org/10.1063/1.5019146

Wierzbicki, E., Kula, D. & Wodzyński, Ł. (2018b). Fourier Variant Homogenization of the Heat Transfer Processes in Periodic Composites. *Mechanics & Mechanical Engineering*, *22* (3), 719–726.

Wierzbicki, E. & Woźniak, C. (2000). On the dynamics of combined plane periodic structures. *Archive of Applied Mechanics*, *70*, 387–398.

Witkowska-Dobrev, J. & Wagrowska, M. (2015). Zasięg efektu warstwy brzegowej w kompozytach warstwowych dla zagadnień elastostatyki. *Acta Scientiarum Polonorum. Architectura*, *14*(2), 3–17.

Wodzyński, Ł., Kula, D. & Wierzbicki, E. (2018). Transport of Temperature Fluctuations Across a Two-Phased Laminate Conductor. *Mechanics & Mechanical Engineering*, *22* (3), 775–787.

Wodzyński, Ł., Kula, D., Wierzbicki, E. (2024). An analysis of the suppression of a pair of odd and even temperature fluctuation in an area occupied by a two-phase one-directional periodically layered composite. *Acta Sci. Pol. Architectura*, *23*, 264–273, DOI: 10.22630/ASPA.2024.23.20

ANALIZA TŁUMIENIA PARZYSTEJ I NIEPARZYSTEJ PARY FLUKTUACJI TEMPERATURY W OBSZARZE ZAJĘTYM PRZEZ DWUFAZOWY JEDNOKIERUNKOWO PERIODYCZNY KOMPOZYT WARSTWOWY

STRESZCZENIE

W pracy analizowane jest zagadnienie zjawiska efektu brzegowego dla dwufazowego kompozytu jednokierunkowo periodycznego i dla wybranych fluktuacji termicznych. Rozważania oparte na równoważnym przeformułowaniu parabolicznego równania przewodnictwa ciepła i rozszerzonym modelu tolerancyjnym prowadzą do wyłonienia optymalnej charakterystyki cech geometrycznych i materiałowych z uwagi na pożądane właściwości izolacyjne. Wprowadzono parametry intensywności tłumienia wykładniczego i rotacyjnego będące miernikami szybkości zanikania i oscylowania fluktuacji brzegowych jako mierniki intensywności zjawiska efektu brzegowego. Zbadano zależność intensywności tłumienia fluktuacji od właściwości geometrycznych i materiałowych przegrody. Przeanalizowano trzy szczególne przypadki par współpracujących fluktuacji.

Słowa kluczowe: efektywne przewodnictwo ciepła, kompozyt periodyczny, efekt brzegowy, rozszerzony model tolerancyjny